Magnetic Field Effects on the Emission from the B State of Gaseous Halogen and Interhalogen Molecules

Takamichi Kobayashi*

Institute for Molecular Science, Myodaiji, Okazaki 444, Japan

Saburo Nagakura†

Graduate University for Advanced Studies, Nagatsuta, Midori-ku, Yokohama 227, Japan

Received: June 2, 1998; In Final Form: August 3, 1998

Magnetic field effects on the emission from the $B^3\Pi_{0^+u}$ state of Br_2 and Cl_2 and the $B^3\Pi_{0^+}$ state of IBr and ICl have been investigated with the aid of excitation spectroscopy under various external magnetic fields up to 7.5 kG. The magnetic quenching was observed for all the investigated vibrational levels of Br_2 and the $v' = 2$ level of IBr, whereas no detectable magnetic quenching was observed for the other levels of IBr and for all the investigated levels of Cl_2 and ICl. The magnetic shortening of emission lifetimes was also observed for Br_2. A linear relationship was found between the magnetic quenching efficiency and the magnetic shortening efficiency. From this it is derived that the former can be represented by the ratio of magnetically induced increment in the nonradiative decay rate to the intrinsic decay rate. This relation can explain the observed dependence of magnetic quenching of Br_2 and IBr upon vibrational and rotational levels. The magnetic quenching efficiency observed for Br_2 and IBr was found to be linearly dependent upon the square of the magnetic field strength. This indicates that the observed magnetic quenching is caused by the direct mechanism.

I. Introduction

External magnetic field effects (MFEs) on the emission of gaseous molecules have been the subject of interest for many decades, and in 1974 Matsuzaki and Nagakura discovered the magnetic quenching of fluorescence from the nonmagnetic singlet excited state of CS_2 vapor.[1] Since then, many polyatomic molecules in their singlet excited states have been found to exhibit MFEs.[2−4] On the other hand, only several diatomic molecules have been known to exhibit magnetic quenching.[5−7] For diatomic molecules, only five molecules are known to exhibit magnetic quenching of emission from their excited states, namely, I_2,[5] Cs_2,[6] Rb_2,[7] NO,[8,9] and CN.[10] Among them, NO and CN are rather special in the sense that specific rotational levels exhibit MFEs through local perturbations.

The mechanism of magnetic quenching of fluorescence is well explained by the theory proposed by Stannard[11] and by Matsuzaki and Nagakura.[12] They proposed that the magnetic field can change the nonradiative transition rate in two different ways, namely, the direct mechanism (DM) and the indirect mechanism (IM). In the DM, two different electronic states with the same spin multiplicity are coupled by the Zeeman perturbation, giving rise to the increase of nonradiative transition rate. In the IM, the intrinsic coupling between electronic states with different spin multiplicity (singlet−triplet interaction, for example) is enhanced because of the field-induced spin decoupling. It is interesting that the DM has been found in only di- and triatomic molecules ($SCCl_2$ is the only exception[13]) and not in larger polyatomic molecules.

Under these circumstances, it is considered to be important to study more systematically and quantitatively the MFEs of small molecules in the gaseous state. In this study, halogen and interhalogen molecules are chosen to study the magnetic quenching. The main purpose is to clarify necessary conditions for the occurrence of magnetic quenching through a systematic comparison of the MFEs of these molecules. In particular, special attention is paid to the relation between magnetic quenching efficiencies and natural lifetimes of emitting levels.

II. Experimental Section

Our experimental setup is schematically shown in Figure 1. A sample cell (Pyrex) is placed at the center of an electromagnet (Tokin SEE-14). The magnetic field strength is varied between 0 and 7.5 kG. An excimer laser (Lambda Physik EMG50E, XeCl, 20 mJ) pumped dye laser (Lambda Physik FL2002) is used as the excitation light source. Coumarin 540A and Rhodamine 610 are used to excite Br_2, and DCM is used for IBr. Coumarin 500 and Coumarin 540A are used for Cl_2 and ICl, respectively. The pulse width, pulse repetition, and line width of the dye laser output are about 10 ns, 10 Hz, and 0.4 cm^{-1}, respectively. Although the spectral resolution was not sufficient to resolve completely rotational lines, lifetimes measured at selected wavelengths are in good agreement with reported values.[14] The Br_2 emission, $B^3\Pi_{0^+u}-X^1\Sigma^+_g$, is monitored with a cutoff filter to eliminate the laser line. The output of a photomultiplier (Hamamatsu Photonics, R928) is fed to a digital storage oscilloscope (Tektronix 2440, 500 MS/s), and digitized data are transferred to a personal computer (EPSON PC-286X) via a GP−IB interface. This computer controls the scan control of the dye laser and the timing of the trigger for the laser.

IBr is appreciably dissociated in equilibrium with I_2 and Br_2. The spectrum of IBr free from I_2 was observed by adding Br_2

* Corresponding author. Present address: National Institute for Research in Inorganic Materials, Namiki, Tsukuba, Ibaraki 305-0044, Japan. E-mail tkobaya@nirim.go.jp; Fax 81-298-51-2768.

†Present address: Kanagawa Academy of Science and Technology, Sakado, Takatsu-ku, Kawasaki 213, Japan.

S1089-5639(98)02446-3 CCC: $15.00
Published on Web 09/09/1998

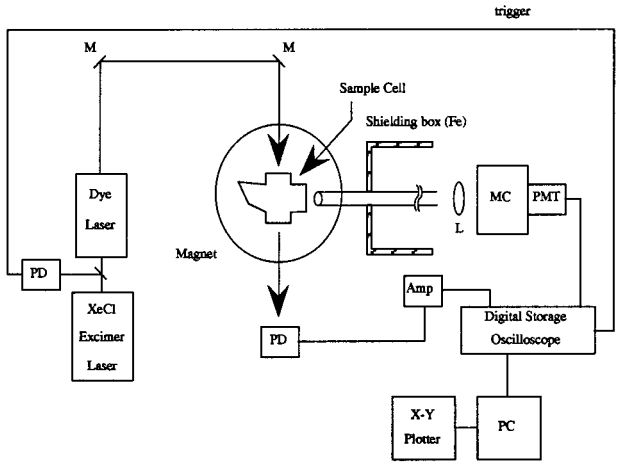

Figure 1. A Schematic diagram of the experimental setup.

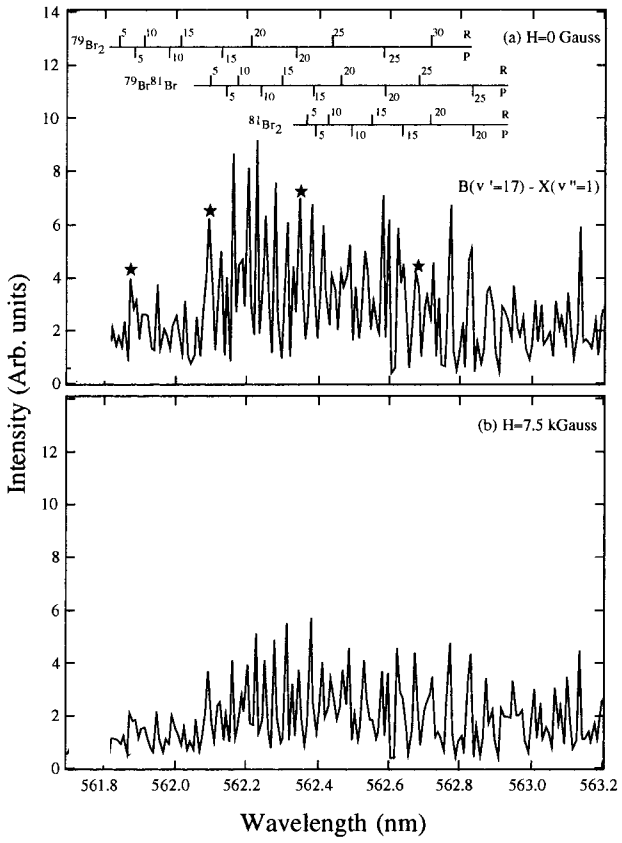

Figure 2. Excitation spectra for the (17−1) band of Br_2 in the presence and absence of a magnetic field (7.5 kG). The vapor pressure is 20 mTorr. Peaks with an asterisk were used for the measurement of magnetic quenching ratios and lifetimes.

to IBr (Br_2, 65 mTorr; IBr, 35 mTorr). In some regions, however, Br_2 lines interfere with IBr lines. In that case, IBr emission was isolated by tuning the monochromator at the resonance fluorescence frequencies of IBr. ICl vapor was sublimed from ICl_3 crystal, which was almost free from I_2.

III. Results and Discussion

III.A. Excitation Spectra and Magnetic Quenching. The excitation spectrum of the B−X transition was observed in the presence and absence of a magnetic field for the (10−2), (14−2), and (17−1) bands of Br_2, for the (3−3) and (2−3) bands of IBr, for the (9−0), (11−0), and (12−0) bands of Cl_2, and for the (2−0), (1−0), (2−3), and (1−2) bands of ICl. Several other bands of Br_2 were also investigated and showed similar behavior to that of the three bands mentioned above. These three bands of Br_2 were chosen for detailed investigation since they were less overlapped with adjacent bands.

TABLE 1: *Q*(*H*) Values Observed for the Three Vibrational Bands Corresponding to the $B^3\Pi_{0^+u} \rightarrow X^1\Sigma^+_g$ Transition of Br_2 (H = 7.5 kG, 5 mTorr Vapor Pressure)[a]

$v' = 17, v'' = 1$				
λ, nm	561.87	562.10	562.35	562.67
$Q(H)$	3.5	2.4	0.9	∼0
$v' = 14, v'' = 2$				
λ, nm	583.28	583.51	583.64	
$Q(H)$	1.1	0.4	∼0	
$v' = 10, v'' = 2$				
λ, nm	600.18	600.35	600.55	
$Q(H)$	2.1	0.8	∼0	

[a] The errors (1 SD) are about 5% of the observed values.

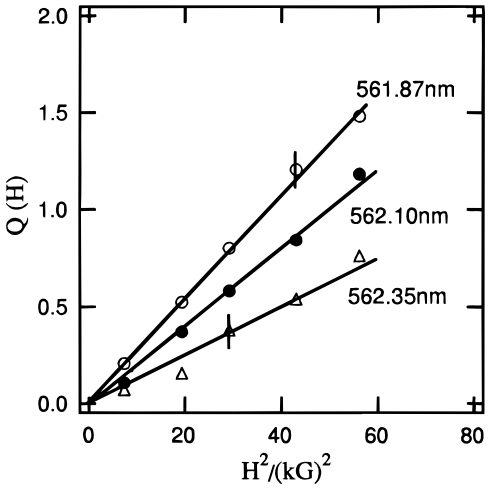

Figure 3. The $Q(H)$ vs H^2 plots for three peaks of the (17−1) band of Br_2 at 20 mTorr. The error bars shown are drawn to ±1 SD, and the errors of other points are about the same as that given by the nearest error bar in the figure.

Typical excitation spectra of Br_2 are shown in Figure 2. From the emission intensity observed under magnetic field strength H, $I(H)$, and that in the absence of magnetic field, $I(0)$, we obtained the magnetic quenching ratio defined as $Q(H) = I(0)/I(H) - 1$, which is the quantitative representation of the magnetic quenching efficiency. The results are shown in Table 1. We can see from the table that the degree of magnetic quenching decreases with increasing wavelength, i.e., higher J'.

The $Q(H)$ values for the (17−1) band were plotted against the square of magnetic field strength in Figure 3. A linear relationship was obtained between both quantities. This is the case for all the investigated bands of Br_2.

Excitation spectra of the (2−3) band of IBr are shown in Figure 4. The magnetic quenching was clearly observed. The (3−3) band of IBr, however, did not exhibit the magnetic quenching. Bands with $v' = 1$ and $v' \geq 4$ were not observed because of the weak emission intensities. Figure 5 shows the magnetic field strength dependence of the magnetic quenching ratio at four peaks: three from the (2−3) band and one from the (3−3) band. The linear dependence of the quenching ratio on the square of magnetic field strength is seen for the (2−3) band. No magnetic quenching was observed for the (3−3) band.

No detectable magnetic quenching was observed for Cl_2 and ICl.

III.B. Lifetimes and Magnetic Quenching of Br_2. Emission lifetimes were measured for some rotation−vibration levels (v' = 17, 14, and 10) of the $B^3\Pi_{0^+u}$ state of Br_2 in the presence

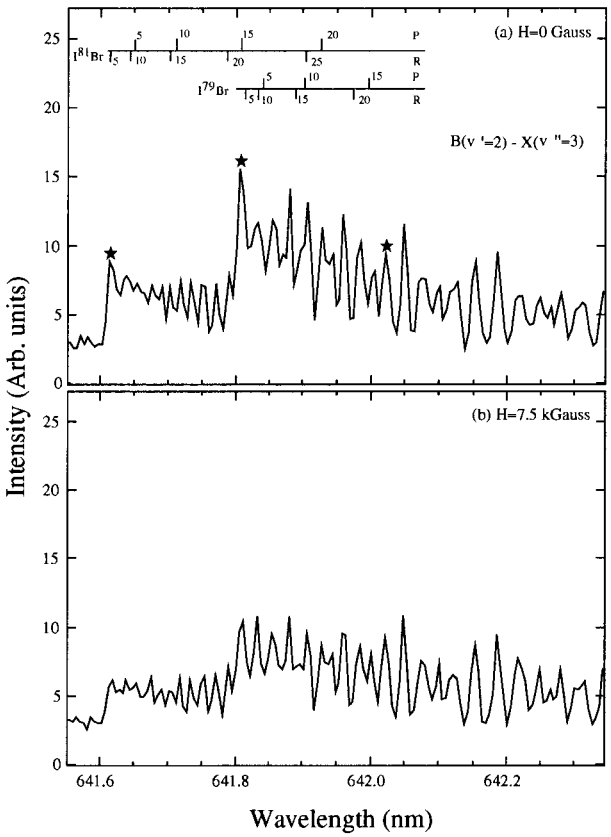

Figure 4. Excitation spectra for the (2−3) band of IBr in the presence and absence of a magnetic field (7.5 kG). The total vapor pressure of IBr and Br_2 is 100 mTorr. Peaks with an asterisk were used for the measurement of magnetic quenching ratios.

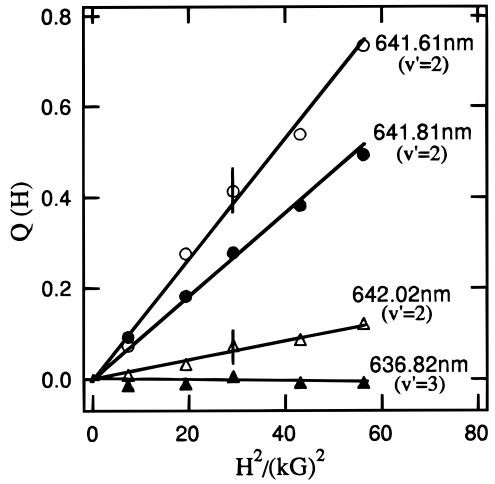

Figure 5. The $Q(H)$ vs H^2 plots for the (2−3) and (3−3) bands of IBr. Three peaks at 641.61, 641.81, and 642.02 nm are taken from the (2−3) band, and a peak at 636.82 nm is from the (3−3) band. The error bars shown are drawn to ±1 SD, and the errors of other points are about the same as that given by the nearest error bar in the figure.

and absence of a magnetic field. Typical decay curves are seen in Figure 6 and show the single-exponential decay. The magnetic shortening of lifetime is clearly seen in the figure. Lifetimes measured in the pressure range 0.01−0.03 Torr satisfied the Stern−Volmer linear relationship. The collision-free lifetimes were obtained by extrapolating the observed ones to zero pressure. The results for the three bands of $v' = 17$, 14, and 10 are summarized in Table 2. For each band, lifetimes were measured at three or four peaks in the region of relatively

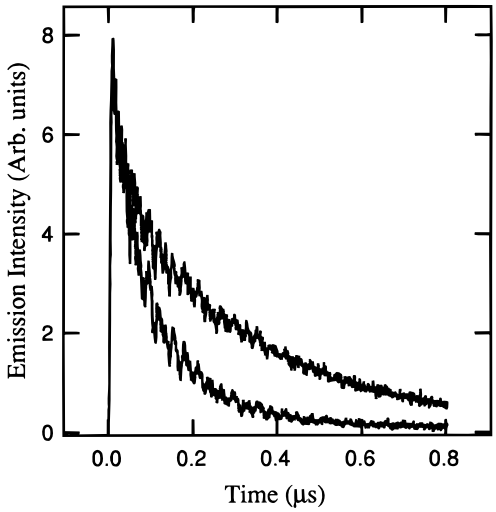

Figure 6. Decay curves for the (17−1) band of Br_2 in the presence (lower trace) and absence (upper trace) of a magnetic field (7.5 kG). Excitation at 561.87 nm. The vapor pressure of Br_2 is 30 mTorr.

TABLE 2: Collision-Free Emission Lifetimes (τ in μs) of the $B^3\Pi_{0^+u}$ State of Br_2 Observed in the Absence and Presence of a Magnetic Field (7.5 kG)[a]

$v' = 17$, $v'' = 1$				
λ, nm	561.87	562.10	562.35	562.67
0 G	1.83	1.4	0.59	0.37
7.5 kG	0.40	0.44	0.42	0.37
$v' = 14$, $v'' = 2$				
λ, nm	583.28	583.51	583.64	
0 G	0.61	0.43	0.36	
7.5 kG	0.39	0.35	0.33	
$v' = 10$, $v'' = 2$				
λ, nm	600.18	600.35	600.55	
0 G	0.88	0.55	0.41	
7.5 kG	0.35	0.29	0.40	

[a] The errors (1 SD) are about 5% of the observed values.

small J' values ($J' < 40$). Table 2 shows that the degree of magnetic shortening of lifetime decreases with decreasing natural lifetime at $H = 0$; i.e., the longer the natural lifetime is, the larger the magnetic shortening.

A comparison of Table 2 with Table 1 indicates that a parallel relationship exists between the magnetic quenching ratio, Q, and the degree of magnetic shortening of lifetime. To illustrate this point more clearly, the observed $Q(H)$ values in Table 1 are plotted against the corresponding ratios of lifetimes, i.e., $\tau(0)/\tau(7.5\text{ kG}) - 1$, derived from the observed lifetimes shown in Table 2. The result is shown in Figure 7. This figure shows that the plots are well represented by a straight line with a slope close to 1; namely,

$$\frac{I(0)}{I(H)} = \frac{\tau(0)}{\tau(H)} \tag{1}$$

The ratio $\tau(0)/\tau(H)$ can be represented by the following equation on the assumption that the back energy transfer processes are negligible.

$$\frac{\tau(0)}{\tau(H)} = \frac{k_H}{k_0} = \frac{k_0 + k_m}{k_0} \tag{2}$$

From eqs 1 and 2

$$Q(H) = \frac{\tau(0)}{\tau(H)} - 1 = \frac{k_m}{k_0} \tag{3}$$

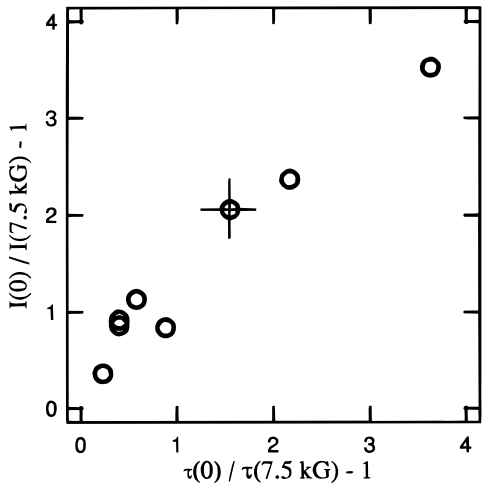

Figure 7. Magnetic quenching ratios vs magnetic shortening ratios of lifetimes for the $B^3\Pi_{0^+u}$ state of Br_2. The error bar shown is drawn to ± 1 SD, and the errors of other points are about the same as the one given in the figure.

where k_0 is the intrinsic decay rate and k_m is the magnetically induced increment in the nonradiative decay rate. Equation 3 shows that the magnetic quenching ratio is determined by the ratio of the magnetically induced increment in the nonradiative decay rate to the intrinsic decay rate of the emitting level. This equation is considered to be applicable to similar simple molecules and to be important in discussing their magnetic quenching.

III.C. Lifetimes and Magnetic Quenching of IBr. As is shown in section III.A, the emission from the $v' = 2$ level of IBr(B) is quenched by external magnetic fields, whereas the emission from the $v' = 3$ level is not quenched. Clyne and Heaven measured the lifetimes of these two vibrational levels of IBr(B).[15] According to their results, the lifetimes of the $v' = 3$ level are much shorter than those of the $v' = 2$ level (roughly by a factor of 5), and all higher vibrational levels ($v' \geq 4$) are completely predissociated. The lifetimes of the $v' = 2$ level of IBr are in the same range as those of Br_2(B). The natural predissociation rate of IBr(B), however, increases very rapidly with increasing v'. According to eq 3, this means that the magnetic quenching efficiency of IBr decreases steeply with increasing v'. This is the reason the magnetic quenching is observed for the emission from the $v' = 2$ level of IBr(B) but not for that from the $v' = 3$ level.

Figures 3 and 5 show that the degree of magnetic quenching decreases with increasing wavelength, i.e., higher J'. According to eq 3, this means that the intrinsic natural lifetime of IBr becomes shorter with increasing J'. This is consistent with the fact that the lifetime of the $v' = 2$ level is strongly dependent on rotational levels and decreases from 3.5 μs for $J' = 7$ to 0.7 μs for $J' = 33$.[15]

From eq 3 and the above-mentioned experimental findings on the magnetic quenching of Br_2 and IBr, it is concluded that the ratio of the magnetically induced increment in the nonradiative decay rate to the intrinsic decay rate is an important factor for observing significant magnetic field effects for small molecules in the gaseous state. It is necessary for observing the magnetic quenching that the latter rate is not too fast, that is to say, the corresponding lifetime long enough. A simple calculation using the observed values in Table 2 provides rough estimates for the intrinsic decay rates (k_0) and the magnetically induced increments in the nonradiative decay rates (k_m). The results are listed in Table 3. Using these decay rates, the magnetic quenching ratios can be calculated by eq 3. Most of the calculated magnetic quenching ratios agree with the corresponding values obtained from the emission intensity measurements (Table 1) within experimental errors except for the case of $v' = 14$ and $v'' = 2$. At 562.67, 583.64, and 600.55 nm at which $Q(H{=}7.5\text{ kG})$ is almost zero, k_m is 1 order or more smaller than k_0.

TABLE 3: Rough Estimates for Decay Rates (in s^{-1}) of the $B^3\Pi_{0^+u}$ State of Br_2 and $Q(H)$ Derived from k_0 and k_m

$v' = 17$				
λ, nm	561.87	562.10	562.35	562.67
k_0	5.5×10^5	7.1×10^5	1.7×10^6	2.7×10^6
k_m (7.5 kG)	2.0×10^6	1.7×10^6	6.8×10^5	0
$Q(H)$	3.6	2.4	0.40	0
$v' = 14$				
λ, nm	583.28	583.51	583.64	
k_0	1.6×10^6	2.3×10^6	2.8×10^6	
k_m (7.5 kG)	9.6×10^5	5.6×10^5	(2.3×10^5)	
$Q(H)$	0.60	0.24	0.08	
$v' = 10$				
λ, nm	600.18	600.35	600.55	
k_0	1.1×10^6	1.8×10^6	2.4×10^6	
k_m (7.5 kG)	1.7×10^6	1.6×10^6	(1.0×10^5)	
$Q(H)$	1.5	0.89	0.04	

III.D. Mechanism of Magnetic Quenching. Figures 3 and 5 show that the magnetic quenching ratio is linearly dependent upon the square of magnetic field strength for all the investigated bands of Br_2 and the $v' = 2$ band of IBr. This is consistent with the theoretical expectation for the magnetic quenching due to the direct mechanism.[11,12] This indicates that the magnetic quenching is caused by the direct mechanism for Br_2.

Baba et al.[16] studied in detail the magnetic quenching of the emission from the $B^3\Pi_{0^+u}$ state of I_2. According to them, the predissociation of the $B^3\Pi_{0^+u}$ state is magnetically enhanced through the mixing with the $2431^1\Pi_u$ state. The mixing occurs through the Zeeman interaction of the $B^3\Pi_{0^+u}$ state with the $2431^3\Pi_{1u}$ component (the direct mechanism) contained in the $2431^1\Pi_u$ state through the spin−orbit interaction. Since the potential energy diagram for I_2 and Br_2 are similar to each other near the $B^3\Pi_{0^+u}$ state, the above mechanism is considered to be applicable to Br_2.

The potential curve of the $B^3\Pi_{0^+}$ state of IBr is somewhat different from that of I_2 or Br_2 because of a strong interaction with the repulsive O^+ state.[17] However, the overall electronic structure of IBr with respect to $B^3\Pi_{0^+}$, $^3\Pi_1$, and $^1\Pi$ states is similar to that of I_2 or Br_2, and there exists a linear dependence of the magnetic quenching ratio upon the square of magnetic field strength for the $v' = 2$ level of IBr. This suggests that the magnetic quenching of IBr is also caused by the direct mechanism.

Acknowledgment. We thank Dr. Minoru Sumitani, Dr. Kaoru Suzuki, and Dr. Haruo Abe for useful suggestions and discussions. This work was partly supported by a Grant-in-Aid for Scientific Research (No. 06740458) from the Ministry of Education, Science, and Culture, Japan.

References and Notes

(1) Matsuzaki, A.; Nagakura, S. *Chem. Lett.* **1974**, 675.
(2) Steiner, U. E.; Ulrich, T. *Chem. Rev.* **1989**, *89*, 51.
(3) Hayashi, H. In *Photochemistry and Photophysics*; Rabek, J. F., Ed.; CRC Press: Boca Raton, FL, 1990; Vol. 1, p 59.
(4) Abe, H.; Hayashi, H. *J. Phys. Chem.* **1994**, *98*, 2797.
(5) Steubing, W. *Verh. Dtsch. Phys. Ges.* **1913**, *15*, 1181.
(6) Kato, H.; Kobayashi, T.; Wang, Y. C.; Ishikawa, K.; Baba, M.; Nagakura, S. *J. Chem. Phys.* **1992**, *162*, 107.
(7) Kato, H. *Faraday Discuss. Chem. Soc.* **1986**, *82*, 1.

(8) Fukuda, Y.; Hayashi, H.; Nagakura, S. *Chem. Phys. Lett*. **1985**, *119*, 480. Sumitani, M.; Abe, H.; Nagakura, S. *J. Chem. Phys*. **1991**, *94*, 1923.
(9) Ottinger, Ch.; Vilesov, A. F. *J. Chem. Phys*. **1994**, *100*, 1805.
(10) Radford, H. E.; Broida, H. P. *J. Chem. Phys*. **1963**, *38*, 644.
(11) Stannard, P. R. *J. Chem. Phys*. **1978**, *68*, 3932.
(12) Matsuzaki, A.; Nagakura, S. *Helv. Chim. Acta* **1978**, *61*, 675.
(13) Abe, H.; Hayashi, H. *Proc. Symp. Mol. Struct., Jpn*. **1993**, 212.
(14) Clyne, M. A. A.; Heaven, M. C. *J. Chem. Soc., Faraday Trans. 2* **1978**, *74*, 1992.
(15) Clyne, M. A. A.; Heaven, M. C. *J. Chem. Soc., Faraday Trans. 2* **1980**, *76*, 49.
(16) Baba, M.; Kimura, M.; Tsuboi, T.; Kato, H.; Nagakura, S. *Bull. Chem. Soc. Jpn*. **1989**, *62*, 17.
(17) Coxon, J. A. In *Molecular Spectroscopy*; Barrow, R. F., Long, D. A., Millen, D. J., Eds.; 1973; Vol. I, p 177.